ELSEVIER

Journal of Magnetic Resonance 165 (2003) 89–94

JMR Journal of Magnetic Resonance

www.elsevier.com/locate/jmr

Dissection of heteronuclear NMR experiments for studies of magnetization transfer efficiencies

D. Braun, K. Wüthrich, and G. Wider*

Institut für Molekularbiologie und Biophysiks, Eidgenössische Technische Hochschule Hönggerberg, Zurich CH-8093, Switzerland

Received 30 April 2003; revised 14 July 2003

Abstract

Modern NMR experiments for applications with biological macromolecules in solution typically include multiple magnetization transfer steps. When working with large structures, a significant fraction of the magnetization is lost during these transfers. For the design and optimization of complex experimental schemes, the magnetization transfer efficiencies have therefore commonly been calculated from the spin relaxation times. This paper now suggests a new method for measurement of individual transfer efficiencies directly with the system of interest, using short, reliable experiments. Initial applications of this approach with a 110,000 Da protein indicate that there is a wide range of transfer efficiencies among individual spin pairs in a structure of this size, which leads to a correspondingly large variation of the individual signal intensities and the need for techniques to enhance the weak signals.

1. Introduction

Knowledge of magnetization transfer efficiencies is one of the foundations of the design of pulse sequences with multiple magnetization transfer steps, and serves quite generally as a basis for optimizing NMR experiments for use with biological macromolecules [1,2]. When working with large structures, fast transverse spin relaxation during transfer steps becomes a major source of signal loss [3]. Conventionally, the magnetization transfer efficiencies have been estimated from the spin relaxation rates. However, the determination of the appropriate relaxation rates is often tedious and inaccurate, especially for rapidly relaxing resonances. In this paper, we present direct measurements of the efficiencies of discrete magnetization transfer steps with the use of short, sensitive experiments, such as one-dimensional (1D) ^{1}H NMR spectra or two-dimensional (2D) heteronuclear correlation experiments. From these data we estimate the measuring times required for obtaining detectable signal intensities in complex multi-dimensional experiments, whereby special consideration is focused on the weak signals typically obtained for well-structured core regions of large protein molecules, or for molecular regions undergoing conformational exchange. As a practical application we studied the magnetization transfers in [^{1}H,^{15}N]-TROSY–HNCO experiments with the protein 7,8-dihydroneopterin aldolase (DHNA) from *Staphylococcus aureus* [4], which has a molecular weight of 110,000 Da.

2. Methods and materials

Magnetization transfer efficiencies, ε, have been measured from comparison of experiments with and without transfer between distinct spin states, and otherwise identical instrument settings, so that ε is the ratio of the integrals of corresponding peaks in the two spectra. For a quantitative comparison of different spectra we used the scaling of the digital Fourier transformation described in [5]

$$S_l = \frac{1}{N}\sum_{k=0}^{N-1} s_k \, e^{-i2\pi kl/N}, \tag{1}$$

where S_l is an individual data point in the frequency domain spectrum, s_k are the time domain data points,

* Corresponding author. Fax: +41-1-6331073.
E-mail address: gsw@mol.biol.ethz.ch (G. Wider).

1090-7807/$ - see front matter © 2003 Elsevier Inc. All rights reserved.
doi:10.1016/S1090-7807(03)00273-8

and N denotes the number of points in the time domain after zero filling. Here, we make use of the well-known fact that the integral over a frequency domain peak represents the amplitude of the first data point in the corresponding FID at the start of the data-acquisition. In a particular experiment j, the magnetization at the start of an evolution period or the detection period can thus be represented by the sum of the intensities of the data points S_l that contribute to the peak r

$$M_j^r = \frac{1}{gnh} \sum S_l. \tag{2}$$

In Eq. (2), g accounts for the receiver gain used, n for the number of scans accumulated, and h for the value of the time domain weighting function at time zero. In writing Eq. (2) it is assumed that the baseline of the spectrum has been set to zero intensity using a baseline correction routine. Eq. (2) affords proper scaling for a direct, quantitative comparison of peak volumes obtained with different experiments. The summation extends over all data points that contribute to the peak r, either in a one-dimensional or a multi-dimensional spectrum. In multi-dimensional experiments, h is the product of the first points of the window functions applied in the different dimensions.

For the determination of the transfer efficiency from spin X to spin Y for a particular transfer element, two experiments are recorded which differ only in that one scheme, i, does and the other scheme, k, does not include this transfer element. For the signal r the transfer efficiency, ε_{XY}^r, is then calculated from the ratio of the magnetizations, M_i^r, and M_k^r

$$\varepsilon_{XY}^r = \frac{M_i^r}{M_k^r}. \tag{3}$$

It is well known that individual commonly used software packages for processing NMR data may apply different scaling during processing of the data (for example, see [6]), and hence care has to be taken to trace the proper scaling of the peak volumes.

A special case of practical interest is obtained when the reference experiment is a 1D ^{1}H NMR spectrum recorded with a sufficiently long interscan delay to reach equilibrium polarization between scans. An identical reference intensity, M_{1D}, is then obtained for all resonances of non-equivalent protons in the spectrum, and M_{1D} can be determined from the peak volume of a well-separated single peak or a well-separated group of peaks, where the volume of the latter has to be divided by the number of resonances contributing to the group. For a signal r, the total magnetization transfer efficiency of any experiment j, E_j^r, can then be defined as the ratio

$$E_j^r = \frac{M_j^r}{M_{1D}}. \tag{4}$$

Using Eq. (4), the overall magnetization transfer efficiency of a given pulse sequence can be assessed for each individual signal r, and the total measuring time required to record data with a predetermined signal-

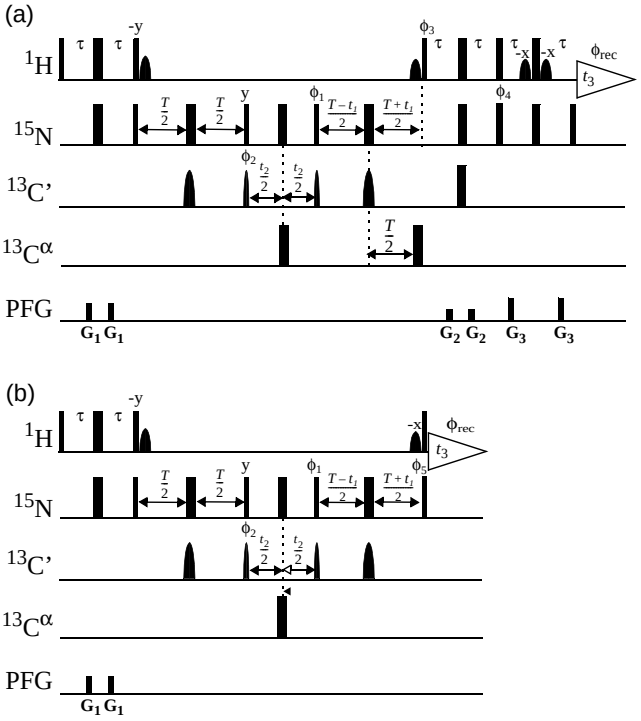

Fig. 1. Experimental schemes of two versions of the 3D [^{15}N,^{1}H]-TROSY–HNCO experiment used in this paper. (a) Conventional experiment with ST2-PT element, in which the delay τ was optimized for maximal signal transfer. The radiofrequency (rf) pulses on ^{1}H, ^{15}N, ^{13}C′, and ^{13}C$^\alpha$ are applied at 4.7, 118, 174, and 55 ppm, respectively. Narrow and wide black bars indicate non-selective 90° and 180° rf pulses. Sine bell shapes on the line marked ^{1}H indicate selective 90° pulses on the water resonance. The use of water flip-back pulses [12] after the initial INEPT transfer and before ϕ_3 ensures that the water magnetization stays aligned along the $+z$-axis throughout the experiment. Bell shapes on the line marked ^{13}C′ represent the center lobe of a sine function; a duration of 120 and 60 μs was used for the 180° and 90° pulses, respectively. The field strength for the ^{13}C$^\alpha$ pulses was 13 kHz. The line marked PFG indicates pulsed field gradients applied along the z-axis with the following durations and strengths: G_1: 500 μs, 24 G/cm; G_2: 500 μs, 16 G/cm; G_3: 200 μs, 40 G/cm. The delay T is set to 17 ms. All rf-pulses are applied with phase x, unless marked otherwise above the pulse bar, with $\phi_1 = \{y,-y,x,-x\}$, $\phi_2 = \{x,x,x,x,-x,-x,-x,-x\}$, $\phi_3 = \{-y\}$, $\phi_4 = \{-y\}$, and $\phi_{rec} = \{y,-y,-x,x,-y,y,x,-x\}$; a phase-sensitive spectrum in the ^{15}N(t_1) dimension was obtained by recording a second FID for each t_1 value, with the phases $\phi_1 = \{y,-y,-x,x\}$, $\phi_3 = \{y\}$, or $\phi_4 = \{y\}$. Quadrature detection in the ^{13}C′(t_2) dimension was achieved by applying the States-TPPI method to ϕ_2 [18]. The data was processed as described in [14]. Residual transverse water magnetization was suppressed by a WATERGATE sequence [19] immediately before data acquisition. (b) The experiment is truncated by omission of the ST2-PT element. Same settings as in (a), except that the phase cycle $\phi_1 = \{x,-x\}$, $\phi_2 = \{x,x,-x,-x\}$, $\phi_5 = \{y\}$, and $\phi_{rec} = \{x,-x,-x,x\}$ is used, and quadrature detection in the ^{15}N(t_1) and ^{13}C′(t_2) dimensions is achieved using the States-TPPI method with phase ϕ_5 and phase ϕ_2, respectively.

to-noise ratio can be estimated from the 1D ^{1}H NMR spectrum of the sample of interest.

As an illustration, the procedure of Eqs. (1)–(4) for the measurement of magnetization transfer efficiencies was applied to a TROSY-type HNCO experiment. The experimental scheme used is shown in Fig. 1a. The original pulse sequence [7] was supplemented by an additional 180° pulse at the carbonyl frequency (last pulse on the line labeled $^{13}C'$ in Fig. 1a) [8]. Based on the analysis of the transfer efficiencies, a truncated version of the experiment is proposed as an alternative for studies of large molecules (Fig. 1b). In this pulse sequence, the ST2-PT element [9] was eliminated so as to obtain a minimal number of transfer steps. In principle, all four multiplet components of an amide moiety will therefore be detected, but in large structures the undesired broad components may be largely suppressed by rapid relaxation [3,10].

For the [^{15}N,^{1}H]-TROSY–HNCO experiment, the relevant magnetization transfer efficiencies were obtained from two pairs of experiments. A 1D ^{1}H NMR spectrum and a 2D [^{1}H,^{15}N]-TROSY spectrum [9,11] acquired with an interscan delay of 16 s were used to determine the transfer efficiency from $^1H^N$ to ^{15}N and back to $^1H^N$, ε^r_{HN}. A 2D [^{1}H,^{15}N]-TROSY spectrum and a 3D-[^{1}H,^{15}N]-TROSY–HNCO experiment recorded with an interscan delay of 2 s (Fig. 1a) were then used to determine the transfer efficiency from ^{15}N to $^{13}C'$ and back to ^{15}N, ε^r_{NC}. In all four experiments, the water was kept along the positive z-axis during most of the pulse sequence and during acquisition [12]. In the 1D ^{1}H NMR experiment, this was achieved using a carefully adjusted $90°_{-x}$ Gaussian-shaped pulse immediately before the $90°_x$ hard excitation pulse.

3. Results

All spectra for the analysis of the transfer efficiencies in a 3D- [^{1}H,^{15}N]-TROSY–HNCO experiment were measured on a Bruker DRX 750 MHz spectrometer at 20 °C. The spectra were obtained with an aqueous solution (pH 6.5) of the homooctameric ^{2}H/^{13}C/^{15}N-labeled dihydroneopterin aldolase from *S. aureus* (DHNA), which has a molecular weight of 110 kDa [4]. The four experiments used to determine the transfer efficiencies ε^r_{HN} and ε^r_{NC} have been described in Section 2. The residue-dependent transfer efficiencies were calculated using Eq. (3). In Fig. 2, the transfer efficiencies from ^{1}H to ^{15}N and back to ^{1}H, ε^r_{HN}, are plotted versus the efficiency of the transfer from ^{15}N to $^{13}C'$ and back, ε^r_{NC}. Most values for ε^r_{HN} lie between 0.1 and 0.01, and for ε^r_{NC} 0.1 and 0.03. The transfer efficiencies ε^r_{HN} and ε^r_{NC} show no obvious correlation, which reflects the large variability of the relaxation rates of individual spins in the 110 kDa protein DHNA. It is noteworthy that the

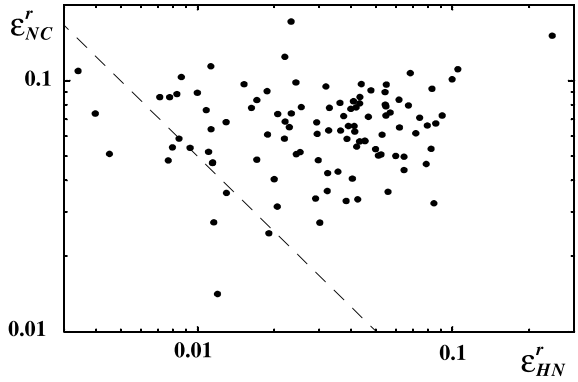

Fig. 2. Plot of magnetization transfer efficiencies from ^{1}H to ^{15}N and back to ^{1}H, ε^r_{HN}, versus the efficiency of the transfer from ^{15}N to ^{13}C and back to ^{13}C, ε^r_{NC}, measured for individual residues in the 110 kDa homooctameric ^{2}H/^{13}C/^{15}N-labeled dihydroneopterin-aldolase from *S. aureus* (DHNA) [4]. Each dot represents the combination of the two transfer efficiencies, ε^r_{HN} and ε^r_{NC}, for a given residue r in the 3D-[^{1}H,^{15}N]-TROSY–HNCO experiment of Fig. 1a with $\tau = 2.7$ ms. Along the straight broken line, the total transfer efficiency is 0.0005.

magnetization transfer efficiencies for individual residues in DHNA vary over about two orders of magnitude.

The presently proposed approach for estimating overall transfer efficiencies depends on various known scaling factors (Eqs. (1) and (2)), which do not depend on knowledge of either the individual transfer efficiencies or the relaxation rates. For a comparison of the new approach and the conventional method using relaxation rates [13], only the C-terminal residue Lys 121 of DHNA could be used. Due to the flexibility of this residue and the resulting intense NMR signals, it was possible to estimate the relaxation rates of its amide moiety from the line widths in the 2D [^{15}N,^{1}H]-HSQC, 2D [^{15}N,^{1}H]-HMQC, and 2D [^{15}N,^{1}H]-TROSY spectra: transverse ^{1}H relaxation rate, $R_2^H = 43\,s^{-1}$; mixed $^1H^N$ and ^{15}N zero- and two-quantum relaxation rate, $R_2^{MQ} = 39\,s^{-1}$; transverse ^{15}N relaxation rate, $R_2^N = 44\,s^{-1}$; transverse relaxation rate for the narrow "TROSY component" of the ^{15}N doublet, $R_2^{NT} = 18\,s^{-1}$. The transfer efficiencies $\varepsilon_{HN}^{Lys121}$ obtained with Eq. (3) and with the conventional method using relaxation rates [13] are 0.28 and 0.25, respectively, and the transfer efficiencies $\varepsilon_{NC}^{Lys121}$ become 0.16 and 0.15, i.e., the values from the two approaches coincide within the error limits.

The measurement of the magnetization transfer efficiencies in the 3D [^{1}H,^{15}N]-TROSY–HNCO experiment showed a substantial loss of magnetization during the transfer between ^{1}H and ^{15}N (Fig. 2), which suggests that for these experiments the length of the transfer period τ should be chosen shorter than the standard value of $1/4J_{NH}$ [2,10]. In TROSY-type experiments, however, the selection of only the most slowly relaxing transition is thereby compromised, and the undesired other multiplet components may show up for $\tau <$

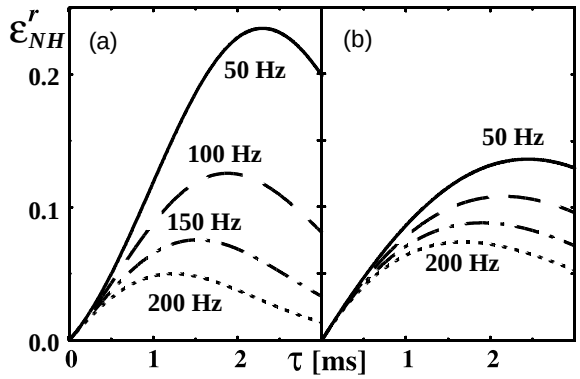

Fig. 3. Calculated efficiencies, ε^r_{HN}, for the magnetization transfer from ^{1}H to ^{15}N and back to ^{1}H versus the length of the transfer delay τ for the two pulse sequences shown in Fig. 1a (a) and Fig. 1b (b), Eqs. (5) and (6) were used, respectively. The transfer efficiencies are shown for four different average transverse relaxation rates $R_2 = (3R_2^H + R_2^N + 2R_2^{MQ})/6$, which are represented by different types of lines: $R_2 = 50\,s^{-1}$ (solid); $R_2 = 100\,s^{-1}$ (long-dash); $R_2 = 150\,s^{-1}$ (dash-dot); and $R_2 = 200\,s^{-1}$ (dot). In (b) the magnetization transfer has been multiplied with a factor of $\sqrt{2}$ to account for the reduced noise in the experiment of Fig. 1b (see text).

$1/4J_{NH}$ [3,9]. However, depending on the actual experimental conditions, the resulting additional peaks may be very weak [10]. The total transfer efficiency for the transfers from ^{1}H to ^{15}N to ^{1}H in a TROSY experiment (Fig. 1a) with τ different from $1/4J_{NH}$ can be estimated with Eq. (5); since the individual relaxation rates R_2^H, R_2^N, and R_2^{MQ} are not known, we use a single exponential with an average relaxation rate R_2

$$\varepsilon^r_{HN} = 0.55\,e^{-6R_2\tau}\sin(2\tau J_{NH}\pi)\left(\frac{\sin(2\tau J_{NH}\pi)+1}{2}\right)^2. \quad (5)$$

In Fig. 3a, ε^r_{HN} is plotted as a function of τ for different values of R_2. For example, using an average transfer efficiency $\varepsilon^r_{HN} = 0.04$ (see Fig. 2) for the signals in the DHNA spectrum, Eq. (5) with $\tau = (4J_{NH})^{-1} \approx 2.7$ ms yields a value for R_2 of approximately $150\,s^{-1}$, which corresponds to an optimal value for τ of about 1.6 ms (Fig. 3a). With this approach the transfer efficiency for the weakest peaks in DHNA can almost be doubled when compared to using $\tau = 2.7$ ms (Fig. 3a). These findings are confirmed by the spectra shown in Figs. 4a and b which were recorded using the ST2-PT element (Fig. 1a) with $\tau = 2.7$ ms (Fig. 4a), and with $\tau = 1.6$ ms, respectively (Fig. 4b). The 2D [^{1}H,^{13}C]-strips in Figs. 4a–c were taken at the amide proton positions of the residues Val 70 to Glu 74, which are located in the core of DHNA. While the rapidly relaxing resonances of Asn 71 and Leu 72 are hardly detectable in Figs. 4a and d both residues are readily detected in the spectrum with $\tau = 1.6$ ms (Figs. 4b and e).

In an alternative, truncated experiment, the ST2-PT element was completely removed (Fig. 1b), so that in principle all four multiplet components of an amide moiety will be observed [3,10]. In very large structures,

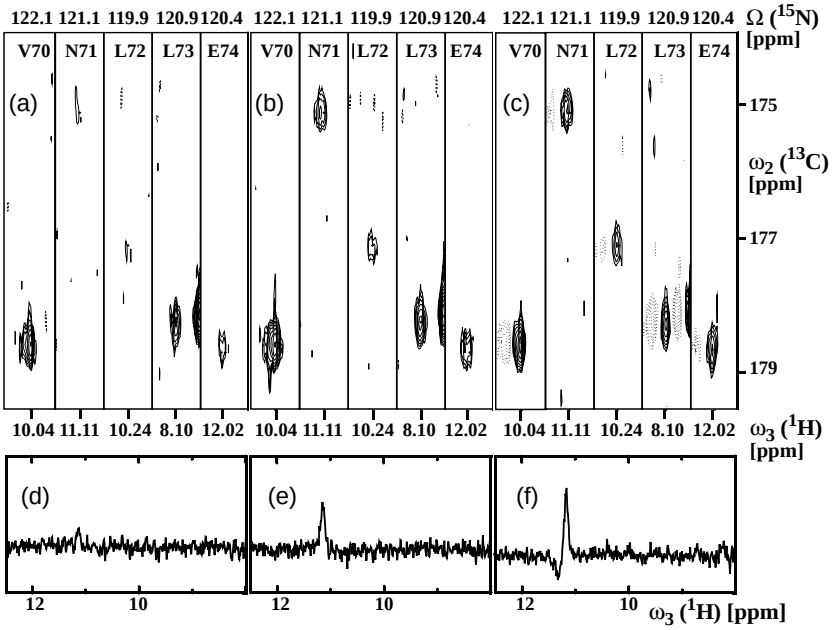

Fig. 4. (a)–(c) $\omega_3(^1H)/\omega_2(^{13}C')$ strips from 3D [^{1}H,^{15}N]-TROSY–HNCO spectra for the residues Val 70 to Glu 74 in the 110 kDa protein DHNA measured at 750 MHz. (a) Experiment of Fig. 1a with $\tau = 2.7$ ms. (b) Experiment of Fig. 1a with $\tau = 1.6$ ms. (c) Experiment of Fig. 1b with $\tau = 1.6$ ms. The interscan delay was set to 2 s, time domain data size 38 (^{15}N) × 30 (^{13}C) × 1024 (^{1}H) complex points, $t_{1,max} = 16$ ms, $t_{2,max} = 12$ ms, and $t_{3,max} = 83$ ms, eight transients were accumulated per $(t_{1,\tau 2})$ value. (d)–(f) Cross sections along the $\omega_3(^1H)$ dimension through the resonance of Asn 71 at $\omega_2(^{13}C) = 175$ ppm from the experiments (a)–(c), respectively.

the broad components will nonetheless be largely suppressed by rapid relaxation [10,15]. This experiment discards half of the ^{15}N magnetization available at the end of the ^{15}N evolution time, and the efficiency of the ^{1}H to ^{15}N to ^{1}H magnetization transfer becomes

$$\varepsilon^{r}_{\mathrm{HN,trunc}} = \frac{0.55}{4}\, e^{-2R_2^{H}\tau} \sin(2\tau J_{NH}\pi). \quad (6)$$

Eq. (6) reflects only the fate of the desired signal but does not take into account the noise in the final spectrum, which is larger by a factor $\sqrt{2}$ for phase-modulated (Fig. 1a) than for amplitude-modulated frequency labeling (Fig. 1b) [2,14]. The magnetization transfer efficiencies plotted in Fig. 3b have therefore been multiplied $\sqrt{2}$ to make the Figs. 3a and b directly comparable with regard to the expected signal-to-noise ratios. Fig. 3 then indicates that for relaxation rates larger than about 150 Hz, the experimental scheme of Fig. 1b should provide higher sensitivity, which is borne out by the experiment in Figs. 4c and f.

4. Discussion

Readily accessible estimates of magnetization transfer efficiencies is an important element of obtaining optimal results from complex NMR experiments with large molecules. Knowledge of the transfer efficiencies allows to optimize the actual pulse sequence and/or to estimate the experimental time for a desired S/N ratio of the signals of interest. The presently proposed direct measurement of discrete magnetization transfer steps by short, sensitive experiments permits even the analysis of very rapidly relaxing signals.

Based on knowledge of the transfer efficiencies, experiments can be better planned. For example, if resonance lines with a particular total transfer efficiency should just be visible in a multi-dimensional NMR experiment, the minimal total number of scans for the whole experiment can be estimated based on a 1D ^{1}H NMR spectrum. Thus, assuming a total transfer efficiency of 0.0005 (broken line in Fig. 2), 2000 times more signal intensity is required for a 3D [^{15}N,^{1}H]-TROSY–HNCO than for a 1D ^{1}H NMR spectrum. Assuming a signal-to-noise value of 20:1 for the resonances of interest in a one-scan 1D ^{1}H spectrum, not less than a total of 10,000 scans will have to be accumulated in order to observe the related signals with 3D [^{15}N,^{1}H]-TROSY–HNCO. Once, the transfer efficiencies for a range of proteins with similar molecular weights will be known, experiment planning may be based on a statistical analysis of the different ranges of known transfer efficiencies, instead of measuring them anew with each protein under investigation.

Another application of transfer efficiencies is the optimization of experiments. The dissection of a TROSY-type HNCO experiment with DHNA revealed a substantial loss of magnetization during the transfer from ^{1}H to ^{15}N (Fig. 2) due to rapid relaxation. Further analysis showed that the length of the transfer period τ (Fig. 1) can be reduced even in TROSY-type experiments, since in large structures the resulting additional peaks [11] are typically very weak. One class of such experiments are the TROSY-type 3D triple-resonance experiments, where the rapidly relaxing line of the ^{15}N-doublet is very efficiently attenuated during the ^{15}N constant time evolution period [8,16]. Appearance of the more rapidly relaxing line of the ^{1}H doublet may be tolerable in 3D spectroscopy, since resonance overlap is usually not severe and the undesired additional resonance line is readily recognizable because of its opposite sign. In principle, this resonance could be suppressed by suitable adjustment of the phase of the last pulse on ^{15}N, which would, however, also slightly reduce the signal of interest [17].

The optimization of the transfer efficiency ε^{r}_{HN} in 3D [^{1}H,^{15}N]-TROSY–HNCO experiments of the 110 kDa protein DHNA is documented in Fig. 4. Among the three experiments shown, the first two were measured with inclusion of the ST2-PT element (Fig. 1a) with $\tau = 2.7$ ms (Fig. 4a) and $\tau = 1.6$ ms (Fig. 4b), respectively, and the third one with the truncated scheme of Fig. 1b with $\tau = 1.6$ ms (Fig. 4c). The truncated scheme shows by far the best sensitivity for the broad resonances. The cross sections through the resonance of Asn 71 (Figs. 4d–f) demonstrate how much sensitivity can be gained for rapidly relaxing resonances from the core of large molecules. When compared to the standard set-up with $\tau = 2.7$ ms, the average intensity of the ten weakest peaks in the 3D [^{1}H,^{15}N]-TROSY–HNCO spectrum of DHNA is increased by a factor of 1.6 ± 0.4 for the experiment with ST2-PT element (Fig. 1a) with $\tau = 1.6$ ms (Fig. 4b), and by 1.9 ± 0.7 for the direct antiphase detection with the scheme of Fig. 1b (Fig. 4c). When all resonances in the DHNA spectrum are considered, the corresponding average gains were 1.5 ± 0.3 and 1.3 ± 0.4, respectively. These signal enhancements apply to all TROSY-type 3D triple resonance experiments that use a constant time ^{15}N evolution period. Here, 3D [^{1}H,^{15}N]-TROSY–HNCO was for practical reasons used as an illustration.

As has been mentioned repeatedly in the text, transfer efficiencies have conventionally been estimated from the relaxation rates. Measurements of the various required relaxation rates are, however, far more time consuming than the technique proposed in the present paper. For example, for a TROSY-type [^{1}H,^{15}N]-correlation experiment, ε^{r}_{HN} would be estimated with [16]

$$\varepsilon^{r}_{HN} = 0.55\, e^{-2R_2^{H}\tau}\left(\frac{e^{-2R_2^{MQ}\tau} + e^{-2R_2^{N}\tau}}{2}\right)\left(\frac{e^{-2R_2^{MQ}\tau} + e^{-2R_2^{H}\tau}}{2}\right), \quad (7)$$

where R_2^{H}, R_2^{N}, and R_2^{MQ} are the transverse relaxation rates for $^1\mathrm{H}^{\mathrm{N}}$, $^{15}\mathrm{N}$, and the mixed zero-quantum and double-quantum state of $^1\mathrm{H}^{\mathrm{N}}$ and $^{15}\mathrm{N}$, respectively. The factor 0.55 in Eq. (7) accounts for the fact that only 50% of the coherence is used during $^{15}\mathrm{N}$ evolution, and that use of the natural $^{15}\mathrm{N}$ polarization yields 10% signal enhancement [9]. The transfer efficiency from $^{15}\mathrm{N}$ to $^{13}\mathrm{C}'$ and back could be calculated with

$$\varepsilon_{\mathrm{NC}}^{r} = 0.5\,\mathrm{e}^{-2R_2^{\mathrm{NT}}T}\sin(TJ_{\mathrm{NC}}\pi)\sin((T+2\tau)J_{\mathrm{NC}}\pi), \qquad (8)$$

where R_2^{NT} is the transverse relaxation rate for the narrow component of the $^{15}\mathrm{N}$ doublet, and J_{NC} the inter-residual scalar coupling between $^{15}\mathrm{N}$ and $^{13}\mathrm{C}'$. The factor 0.5 accounts for the fact that the chemical shift evolution of the $^{15}\mathrm{N}$ magnetization is measured with amplitude modulation, which causes a loss of on average 50% of the magnetization.

Acknowledgment

We thank M. Salzmann for providing us with a DHNA sample.

References

[1] A. Bax, S. Grzesiek, Methodological advances in protein NMR, Acc. Chem. Res. 26 (1993) 131–138.
[2] G. Wider, Technical aspects of NMR spectroscopy with biological macromolecules and studies of hydration in solution, Prog. NMR Spectrosc. 32 (1998) 193–275.
[3] R. Riek, G. Wider, K. Pervushin, K. Wüthrich, Polarization transfer by cross-correlated relaxation in solution NMR with very large molecules, Proc. Natl. Acad. Sci. USA 96 (1999) 4918–4923.
[4] M. Hennig, A. D'Arcy, I. Hampele, M. Page, C. Oefner, G. Dale, Crystal structure and reaction mechanism of 7,8-dihydroneopterin aldolase from *Staphylococcus aureus*, Nature Struct. Biol. (1998) 357–362.
[5] R.R. Ernst, G. Bodenhausen, A. Wokaun, Principles of Nuclear Magnetic Resonance in One and Two Dimensions, Oxford Science Publications, Clarendon Press, Oxford, 1987, p. 105.
[6] J. Cavanagh, W.J. Fairbrother, A.G. Palmer III, N.J. Skelton, Protein NMR Spectroscopy, Principles and Practice, Academic Press, San Diego, 1996, p. 105.
[7] M. Salzmann, K. Pervushin, G. Wider, H. Senn, K. Wüthrich, TROSY in triple-resonance experiments: new perspectives for sequential NMR assignment of large proteins, Proc. Natl. Acad. Sci. USA 95 (1998) 13585–13590.
[8] M. Salzmann, G. Wider, K. Pervushin, K. Wüthrich, Improved sensitivity and coherence selection for [^{15}N,^{1}H]-TROSY elements in triple resonance experiments, J. Biomol. NMR 15 (1999) 181–184.
[9] K.V. Pervushin, G. Wider, K. Wüthrich, Single transition-to-single transition polarization transfer (ST2-PT) in [^{15}N,^{1}H]-TROSY, J. Biomol. NMR 12 (1998) 345–348.
[10] R. Riek, J. Fiaux, E.B. Bertelsen, A.L. Horwich, K. Wüthrich, Solution NMR techniques for large molecular and supramolecular structures, J. Am. Chem. Soc. 124 (2002) 12144–12153.
[11] K. Pervushin, R. Riek, G. Wider, K. Wüthrich, Attenuated T_2 relaxation by mutual cancellation of dipole–dipole coupling chemical shift anisotropy indicates an avenue to NMR structures of very large biological macromolecules in solution, Proc. Natl. Acad. Sci. USA 94 (1997) 12366–12371.
[12] S. Grzesiek, A. Bax, The importance of not saturating H_2O in protein NMR. Application to sensitivity enhancement and NOE measurements, J. Am. Chem. Soc. 115 (1993) 12593–12594.
[13] M. Rance, J.P. Loria, A.G. Palmer III, Sensitivity improvement of transverse relaxation-optimized spectroscopy, J. Magn. Reson. 136 (1999) 92–100.
[14] L.E. Kay, P. Keifer, T. Saarinen, Pure absorption gradient enhanced heteronuclear single quantum correlation spectroscopy with improved sensitivity, J. Am. Chem. Soc. 114 (1992) 10663–10664.
[15] J. Fiaux, E.B. Bertelsen, A.L. Horwich, K. Wüthrich, Interactions of GroES with GroEL in a 900 kDa chaperonin complex mapped by NMR in solution, Nature 418 (2002) 207–211.
[16] D. Yang, L.E. Kay, Improved $^1\mathrm{H}^{\mathrm{N}}$-detected triple resonance TROSY-based experiments, J. Biomol. NMR 13 (1999) 3–10.
[17] T. Schulte-Herbrüggen, O.W. Sorensen, TROSY: compensation for relaxation-induced artifacts, J. Magn. Reson. 144 (2000) 123–128.
[18] D. Marion, M. Ikura, R. Tschudin, A. Bax, Rapid recording of 2D NMR spectra without phase cycling. Application to the study of hydrogen exchange in proteins, J. Magn. Reson. 85 (1989) 393–399.
[19] M. Piotto, V. Saudek, V. Sklenár, Gradient-tailored excitation for single-quantum NMR spectroscopy of aqueous solutions, J. Biomol. NMR 2 (1992) 661–665.